AEI–2004–065
IGPG-04/8-2

Time dependence in Quantum Gravity

Martin Bojowald*

Max-Planck-Institut für Gravitationsphysik, Albert-Einstein-Institut,

Am Mühlenberg 1, D-14476 Potsdam, Germany

Parampreet Singh†

Institute for Gravitational Physics and Geometry,

Pennsylvania State University, University Park, PA 16802, USA

Aureliano Skirzewski‡

Max-Planck-Institut für Gravitationsphysik, Albert-Einstein-Institut,

Am Mühlenberg 1, D-14476 Potsdam, Germany

Abstract

The intuitive classical space-time picture breaks down in quantum gravity, which makes a comparison and the development of semiclassical techniques quite complicated. By a variation of the group averaging method to solve constraints one can nevertheless introduce a classical coordinate time into the quantum theory, and use it to investigate the way a semiclassical continuous description emerges from discrete quantum evolution. Applying this technique to test effective classical equations of loop cosmology and their implications for inflation and bounces, we show that the effective semiclassical theory is in good agreement with the quantum description even at short scales.

PACS numbers: 04.60.Pp,04.25.-g,98.80.Qc

* e-mail address: mabo@aei.mpg.de
† e-mail address: singh@gravity.psu.edu
‡ e-mail address: skirz@aei-potsdam.mpg.de

I. INTRODUCTION

Current knowledge of the quantum structure of space-time suggests a picture very different from the smooth classical one. Space and time are expected to be fundamentally discrete such that both change only in steps. Still, a transition between both pictures must be possible in order to understand the emergence of a classical world on large scales from the fundamental quantum world. Also for practical purposes such a transition is helpful in a semiclassical approximation.

A technically and conceptually important question is where the classical picture starts to make sense or, when going to smaller and smaller scales, where it breaks down. The change of scale can happen either computationally, i.e. by looking at smaller and smaller scales in a coarse-grained approximation which can then be used, for instance, to understand the breaking or deformation of classical symmetries, or dynamically during the expansion or contraction of a universe or the collapse of matter to a black hole.

One application is the behavior of universes which on larger scales has been studied from the point of view of loop quantum cosmology [1, 2] by using effective classical equations [3, 4, 5, 6]. While the fundamental description is quantum, governed by a difference equation for the wave function [7, 8, 9], effective classical equations show the diverse cosmological effects more easily. The idea of using effective classical equations is that in semiclassical regimes they describe the position of wave packets solving the difference equation. They simplify the analysis considerably even in isotropic models and can be expected to do so even more in inhomogeneous models or the full theory. In light of the previous discussion an open question is where exactly an effective classical equation makes sense as a good approximation to the behavior of the difference equation, and where additional correction terms have to be taken into account. This is of relevance also for cosmology, for instance in order to determine the starting point of inflation [3, 10, 11, 12], observable signatures in CMB [10], the validity of effective classical bounce pictures [13, 14, 15, 16, 17], or general aspects of the approach to a classical singularity [18, 19].

A particularly striking difference between the classical and the quantum theory is the issue of time. A common understanding which works in both cases is that of relational time, where time is not an external, absolute parameter but encoded in the relative change between different degrees of freedom [20, 21, 22]. However, this concept is difficult to use explicitly,

and so classically one employs the space-time picture where time is just a gauge coordinate. Thus, this time coordinate has no invariant physical meaning, but nevertheless provides a helpful intuitive understanding of a given gravitational system. From the Hamiltonian point of view, this time coordinate is the gauge parameter for orbits generated by the Hamiltonian constraint. In this way, coordinate time is related to the second effect of a first class classical constraint, namely that of generating a gauge transformation in addition to restricting fields to the constraint surface.

In a canonical quantum theory the situation is different because in the Dirac procedure to solve first class constraints there is only one step by requiring physical states to be annihilated by the quantum constraints, which then are automatically gauge invariant. In systems with a Hamiltonian constraint, physical states are thus timeless, which has lead to the name 'frozen formalism.' As we will discuss below, the two steps familiar from the classical procedure can easily be disentangled also in a quantum procedure to solve the constraints, in particular if the technique of group averaging [23] is used. Physical states can then be represented as evolving histories, which are dependent on the gauge choice via the lapse function. At a given time parameter of the history the constraints will not be satisfied but the whole history represents a physical state in a well-defined way.

Practical applications are obtained as a scheme to decide where effective classical equations can be used, and which correction terms should be included. To that end, we compare the expectation value of, e.g., the volume in a given time dependent quantum state with the classical volume or that obtained from a classical equation with correction terms. Those correction terms can be derived by computing the expectation value of the Hamiltonian constraint operator in a coherent state and expanding around the classical expression [24, 25]. There are diverse sources of deviations in the case of non-linear constraints which can be studied analytically or numerically: First, there are the usual Ehrenfest statements about the relation between classical and quantum equations of motion for expectation values. In addition there are choices related to choosing an initial semiclassical state, and the way the constraints are violated at fixed coordinate times. Finally and most importantly, there are genuine quantum gravity corrections whose implications can give rise to new physical effects.

As we will see, it is possible to disentangle those effects at least qualitatively. The resulting modifications to classical behavior can then be compared to known analytical results, as done here for inflationary behavior and bounces, or be used to suggest new effects. In the next

section we recall the group averaging procedure which will be followed by a brief discussion of the issue of time in this context. In Sec. IV we will present a way to implement this idea numerically and study examples of universes with a cosmological constant or dust as matter. We will show that, both for inflation and bounces, the effective semiclassical theory which incorporates modified geometrical densities is in good agreement with discrete quantum evolution till very small scales. This proves that effects derived from the effective semiclassical theory capture to a large extent the true nature of quantum spacetime. Here we focus on describing the way our technique can prove useful in testing a semiclassical theory, leaving a more detailed study for future work.

II. GROUP AVERAGING

We will discuss here only systems with a single constraint which we mostly think of as a Hamiltonian constraint generating coordinate time. In an isotropic cosmological model the constraint itself will be the Friedmann equation, and the evolution equation it generates is the Raychaudhuri equation plus equations for matter fields such as the Klein–Gordon equation for a scalar. After quantizing we obtain the constraint operator which annihilates physical states, and all evolution would have to be extracted from physical states in a relational way.

A simple method to implement a constraint on quantum states is as follows. Consider the action of the constraint operator $\hat{C}$ on a given non-physical state interpreted to promote a change in gauge parametrized by a real parameter λ

$$\hat{C}\,|\varphi_\lambda\rangle = i\frac{\mathrm{d}}{\mathrm{d}\lambda}\,|\varphi_\lambda\rangle\ . \tag{1}$$

Obviously $|\varphi_\lambda\rangle$ is not annihilated by the operator $\hat{C}$ unless $|\varphi_\lambda\rangle$ is independent of λ, i.e. gauge invariant. To achieve λ-independence we can average the state $|\varphi\rangle \equiv \int \mathrm{d}\lambda\,|\varphi_\lambda\rangle$ such that

$$\hat{C}\,|\varphi\rangle = \int \mathrm{d}\lambda\,\hat{C}\,|\varphi_\lambda\rangle = i\int \mathrm{d}\lambda\,\frac{\mathrm{d}}{\mathrm{d}\lambda}\,|\varphi_\lambda\rangle \tag{2}$$

which in the case of compact symmetry orbits or suitable boundary conditions in the non-compact case vanishes identically. In conclusion, we can get a solution to our constraint by averaging the nonphysical state over the symmetry group: $\int \mathrm{d}\lambda\,|\varphi_\lambda\rangle$. This is in fact not new because the solution to our equation for a state $|\varphi\rangle_\lambda$ is given by

$$|\varphi_\lambda\rangle = e^{-i\lambda\hat{C}}\,|\varphi\rangle_0 \tag{3}$$

and the invariant state is

$$\int \mathrm{d}\lambda\, e^{-i\lambda\hat{C}}\,|\varphi\rangle \tag{4}$$

which is nothing else than the group averaging map [23] into the physical Hilbert space.

As examples we consider different cases in which the method works with different success. The simplest case would be to consider the constraint $\hat{P}_\theta\,|\varphi\rangle = 0$ which imposes rotation invariance on a two dimensional system with angular coordinate θ. Then, by following the prescription presented above we replace the equation

$$\langle\theta|\,\hat{P}_\theta\,|\varphi\rangle = i\,\partial_\theta\varphi(\theta) = 0 \tag{5}$$

with a Schrödinger like equation. The constraint then acts on non-physical states by

$$i\,\partial_\theta\varphi_\lambda(\theta) = i\,\partial_\lambda\varphi_\lambda(\theta) \tag{6}$$

with general solution

$$\varphi_\lambda(\theta) = \varphi(\lambda+\theta)\,. \tag{7}$$

Physical states are thus given by

$$\varphi = \int_0^{2\pi}\mathrm{d}\lambda\,\varphi(\lambda+\theta) = \int_0^{2\pi}\mathrm{d}\lambda\,\varphi(\lambda) \tag{8}$$

where any θ-dependence is removed.

We can also consider the non compact case by using the translation generator $\hat{P}_x$ with exactly the same calculations (except that allowed functions φ have to be restricted to a suitable set for the λ-integration to exist, similarly to selecting an appropriate subspace of the kinematical Hilbert space for group averaging). For a more general example let us consider the operator $\hat{C} = a\hat{X}\hat{P} + b$ to follow the strategy above, i.e. use the operator to generate transformations of an arbitrary state, and then solve the resulting partial differential equation. In this case the equation becomes

$$(a\,x\,i\partial_x + b)\,\varphi_\lambda(x) = i\partial_\lambda\varphi_\lambda(x) \tag{9}$$

with solution

$$\varphi_\lambda(x) = e^{\frac{ib}{2}(\frac{1}{a}\ln(x)-\lambda)}f(\ln(x)/a+\lambda). \tag{10}$$

Then, in order to realize the λ integration we Fourier transform $f(\frac{1}{a}\ln(x)+\lambda)$ which is possible only for a real: $f(u) = (2\pi)^{-1}\int_{-\infty}^{\infty}\mathrm{d}\omega e^{-i\omega u}\tilde{f}(\omega)$. Moreover, we commute the λ- and

ω-integrations,

$$\int_{-\infty}^{\infty} \mathrm{d}\lambda \varphi_\lambda(x) = e^{i\frac{b}{2}\frac{1}{a}\ln(x)} \int_{-\infty}^{\infty} \frac{\mathrm{d}\omega}{2\pi}\, e^{-i\omega\frac{1}{a}\ln(x)} \tilde{f}(\omega) \int_{-\infty}^{\infty} \mathrm{d}\lambda\, e^{-i(\omega+\frac{b}{2})\lambda}\,. \tag{11}$$

Here, the integral in λ would diverge for arbitrary complex b and we get a solution for the constraint only if it is real. After integrating over λ and ω we obtain $\varphi(x) = ce^{i\frac{b}{a}\ln(x)}$ which can be checked to satisfy our constraint. If $b \notin \mathbb{R}$, the final integration diverges which means that we are not allowed to commute the integrations. Moreover, in this case we would have to choose appropriate fall-off conditions for f.

Whether or not we are using a self-adjoint constraint operator has significance for the physical inner product, which we are not considering here. Still, adjointness properties also play a role at the level of solving the constraint, as the following example given by $\hat{C} = \partial/\partial x$ demonstrates. Now we have to solve the equation

$$\partial_x \varphi_\lambda(x) = i\,\partial_\lambda \varphi_\lambda(x)$$

which is done by any arbitrary function $\varphi_\lambda(x) = \varphi(\lambda + ix)$ depending only on $\lambda + ix$. Integrating over λ to compute a physical state is now done along a line shifted vertically by the amount x in the complex plane, where we interpret solutions $\varphi_\lambda(x)$ as holomorphic functions on the complex plane with coordinate $z = \lambda + ix$. The result will be independent of x only if φ satisfies appropriate fall-off conditions and does not have residues. Both properties together cannot be satisfied for non-zero functions since, owing to Liouville's Theorem any bounded entire function is constant. Thus, any function for which the λ-integrations exist must have poles on the complex plane such that the averaging procedure does not lead to constant functions of x, as expected for this constraint, but only to locally constant ones.

While the averaging can be defined even for non-selfadjoint constraints, from the numerical point of view self-adjointness of the constraint operator is essential. Non-real eigenvalues would imply exponentially growing modes in solutions to the differential equation which lead to numerical instabilities.

III. COORDINATE TIME

Quantum gravity in the perspective of canonical quantization arises as a constrained system which gives rise to the well known Wheeler–DeWitt equation instead of a Schrödinger

like equation. Nowadays canonical quantum gravity is usually formulated with Ashtekar variables and it is possible to realize the constraint algebra on a well-defined kinematical Hilbert space [26, 27, 28, 29, 30]. The Gauss and diffeomorphism constraints can be solved by group averaging [26], but discussions about the correct Hamiltonian constraint are not settled yet [27, 30, 31]. Also the issue of the physical inner product and how to use the solution space to the Hamiltonian constraint are almost completely open in the full theory. After reducing to symmetric models [32], the Hamiltonian constraint simplifies and can often be treated explicitly. Even in the simplest cosmological models the physical inner product is not yet understood, but since the spatial volume can be used as internal time in a cosmological situation the problem of time does not play a role. In all these cases there is a Hamiltonian constraint whose gauge parameter classically corresponds to coordinate time, and it is our aim to discuss how such a parameter can appear with this interpretation in quantum theory.

As discussed before, the group averaging procedure to solve constraints can be split into two steps which roughly correspond to the two classical steps of restricting to the constraint surface and factoring out by the gauge orbits. The correspondence is not perfect, however, since one single member φ_{λ_0} of a family $\{\varphi_\lambda\}_{\lambda\in\mathbb{R}}$ of states exhibiting the gauge parameter is not a solution to the quantum constraint, while a classical gauge orbit can completely lie within the constraint surface. Even in a semiclassical regime this would lead to deviations between the classical and quantum behavior since the constraints are always violated when the gauge parameter is exhibited. Still, as an approximation and a heuristic tool the gauge dependent family of states can be very useful. In particular for the Hamiltonian constraint of a gravitational system this allows us to describe the quantum theory approximately with reference to a coordinate time, which justifies the use of effective classical equations of motion.

Taking into account possible choices of lapse functions, which after quantizing can be operators if N depends on t via kinematical degrees of freedom (such as $N(t) = a(t)$ which is used when transforming from proper time to conformal time in an isotropic model), we arrive at

$$\hat{N}\hat{H}\,|\Psi_t\rangle = i\frac{\mathrm{d}}{\mathrm{d}t}\,|\Psi_t\rangle \tag{12}$$

as the evolution specified by the Hamiltonian constraint operator.

The condition that the Hamiltonian constraint has to annihilate physical states empha-

sizes the fact that physics does not depend on (coordinate) time. Correspondingly, Eq. (12) which is directly related to a choice of time through a Schrödinger equation on non physical states is in fact not unique because we can fix the gauge freedom in different ways by making different choices of the quantized version $\hat{N}$ of the lapse function.

IV. APPLICATIONS

For semiclassical physics it is very convenient to have an explicit coordinate time parameter since classical intuition is based on the space-time picture. In principle it is also possible to work with internal times both at the quantum and classical level, but it comes with much more technical effort. In the case of loop quantum cosmology, in fact, most recent phenomenological applications [3, 5, 10, 11, 12, 13, 14, 15, 16, 17, 18, 19] are based on effective classical equations [3, 4] which are differential equations in coordinate time and implement the main non-perturbative quantum effect [33, 34] in matter Hamiltonians [35]. Direct studies of the underlying difference equations, on the other hand, are more complicated [36, 37, 38, 39, 40].

These equations show the main qualitative effects that have to be expected from the loop quantization at a more intuitive level. For more quantitative applications, however, it is important to see to which degree they provide an approximation to the quantum behavior and whether in some regimes additional correction terms have to be taken into account. Those additional correction terms can, for instance, be obtained from computing the expectation value of the constraint operator in a coherent state [24, 25]. This results in the classical constraint together with correction terms, and thus corrected equations of motion for, e.g., the scale factor. The present paper suggests an alternative procedure, which is one step closer to the quantum theory. Using the quantum coordinate time picture, we can evolve the state first within the quantum theory, and then compute the expectation value of, e.g., the volume operator which also gives us the time dependence of the scale factor. Both procedures are approximations to the quantum dynamics: In the first case one uses kinematical coherent states to compute the expectation value, while in the second case coordinate time is introduced which, as explained above, is not exact in quantum theory. In both cases, however, the Hamiltonian constraint is used and implemented at least partially: The first case imposes a classical constraint with quantum corrections, while in the second

the quantum constraint is used to evolve states, which then could be averaged if we are interested in the physical state.

In a sense, the procedures differ by a commutation of evolving and translating from quantum to classical behavior (by taking expectation values). We either take the expectation value of the constraint first (in a kinematical coherent state) and then determine the evolution in a classical manner, or we first evolve a kinematical state with quantum operators and then determine classical quantities from expectation values in the resulting, time-dependent states. It is not guaranteed that the two different steps in fact commute, which leads to differences between the two procedures. In simple models, however, both ways of determining the dynamics can be implemented at least numerically and then compared with each other. We will demonstrate this in what follows, leaving a more detailed investigation with precise statements of ranges of applicability and of the necessity of additional correction terms for future work.

A. Numerical implementation

In isotropic loop quantum cosmology for a flat model, the Hamiltonian constraint operator is given by [8, 24]

$$\begin{aligned}(\hat{H}_0\tilde{\psi})_\mu &= (V_{\mu+5}-V_{\mu+3})\tilde{\psi}_{\mu+4}-2(V_{\mu+1}-V_{\mu-1})\tilde{\psi}_\mu\\ &\quad +(V_{\mu-3}-V_{\mu-5})\tilde{\psi}_{\mu-4}+\tfrac{8}{3}\pi G\gamma^3\ell_{\mathrm{P}}^2\ \mathrm{sgn}(\mu)\hat{H}_{\mathrm{matter}}(\mu)\tilde{\psi}_\mu\end{aligned}$$

acting on a wave function $\tilde{\psi}\colon \mathbb{R}\to\mathbb{C}$ supported on eigenspace of the triad operator $\hat{p}$. The coefficients are given in terms of the volume eigenvalues $V_\mu = (\frac{1}{6}\gamma\ell_{\mathrm{P}}^2)^{3/2}|\mu|^{3/2}$, with the Barbero–Immirzi parameter $\gamma = 0.238$ [41] as it follows from calculations of black hole entropy [42, 43], and $\hat{H}_{\mathrm{matter}}(\mu)$ is the matter Hamiltonian which we will choose later.

Since only labels distances of four apart are involved, we introduce $4m := \mu$ with integer m (see also [44] for this restriction) and write the operator as

$$\begin{aligned}(\hat{H}_0\psi)_m &= (v_{m+5/4}-v_{m+3/4})\psi_{m+1}-2(v_{m+1/4}-v_{m-1/4})\psi_m\\ &\quad +(v_{m-3/4}-v_{m-5/4})\psi_{m-1}+\tfrac{8}{3}\pi G\gamma^3\ell_{\mathrm{P}}^2\ \mathrm{sgn}(m)\hat{H}_{\mathrm{matter}}(4m)\psi_m\end{aligned}$$

with $\psi_m := \tilde{\psi}_{4m}$ and $v_m := V_{4m}$. This operator will have to be symmetrized to $\hat{H} := \frac{1}{2}(\hat{H}_0 + \hat{H}_0^\dagger)$ for group averaging and the implementation of coordinate time to apply numerically.

(Alternatively, we can choose a lapse function $N(t) = a(t)$, corresponding to conformal time, and quantize such that $\hat{N}$ has eigenvalues proportional to $V_{\mu+1} - V_{\mu-1}$. The resulting operator $\hat{N}\hat{H}_0$ would be symmetric without reordering $\hat{H}_0$, but since the lapse function and its quantization vanish for $a = 0$, the quantum behavior around $\mu = 0$ will be problematic.) Moreover, for numerical purposes we need to restrict the operator to finite lattices $\mathcal{L}_{m_c,N} := \{n \in \mathbb{Z} : m_c - N/2 < m \leq m_c + N/2\}$ of size N and centered at m_c, such that it will be represented by a tridiagonal $N \times N$-matrix H_{ij} with $H_{ij} = 0$ for $j > i + 1$ or $i > j + 1$,

$$H_{ii} = -2(v_{m_c-N/2+i+1/4} - v_{m_c-N/2+i-1/4}) + \tfrac{8}{3}\pi G\gamma^3\ell_{\mathrm{P}}^2 \operatorname{sgn}(m_c - \tfrac{1}{2}N + i)\hat{H}_{\mathrm{matter}}(m_c - \tfrac{1}{2}N + i) \tag{13}$$

and

$$H_{i,i+1} = H_{i+1,i} = \tfrac{1}{2}(v_{m_c-N/2+i+5/4} - v_{m_c-N/2+i+3/4} + v_{m_c-N/2+i+1/4} - v_{m_c-N/2+i-1/4})\,. \tag{14}$$

We now introduce the coordinate time parameter t and solve

$$H \cdot \psi_t = i\,\frac{\mathrm{d}}{\mathrm{d}t}\psi_t \tag{15}$$

numerically. The solution to the differential equation (15) is then given by

$$\psi_t = \exp(-itH) \cdot \psi_{\mathrm{in}}$$

with an initial state $\psi_{\mathrm{in}} \in \mathbb{C}^N$. The function ψ_t can then be used to compute time dependent expectation values.

B. Examples

As examples of our technique, we first consider the case where the scale factor is the sole degree of freedom, i.e. we do not couple a matter field. Unlike with an internal time evolution, for which no other degree of freedom besides internal time a would be left, this still allows us to have a non-trivial evolution of a in coordinate time t. This is followed by examples of inflation and bounce with inclusion of matter (dust) in the analysis which signifies the role played by effective densities in a good semiclassical description.

1. Effective classical behavior

The main choice to be made in order to study the coordinate time evolution of a given system is the initial state ψ_{in} which in our case is a function on a discrete lattice. It should

be peaked on a specified classical volume, together with an extrinsic curvature which follows from the volume and the classical Hamiltonian constraint. A quantum theory, of course, allows much more freedom in choosing the initial state, and we will simply use a Gaussian

$$\psi_{\mathrm{in},j} = \exp\left(-\frac{(j-N/2)^2}{4\sigma^2} + 2i(j-N/2)c_0\right)$$

in what follows, where the isotropic connection component c_0, related to extrinsic curvature by $c = -\gamma\dot{a}/2$, is determined from the peak scale factor $a_0 = \sqrt{\frac{2}{3}\gamma\ell_{\mathrm{P}}^2|m_c|}$ [49] by the constraint $-6c_0^2a_0 + 8\pi G\gamma^2 H_{\mathrm{matter}}(a_0) = 0$. (At this point the classical equations to be compared with enter. If correction terms are included, as will be done later, the value of c_0 changes and so does the quantum evolution of the new initial state.) Nevertheless, the explicit choice has an influence on the evolution such as the degree of spreading of the wave packet. Numerically, a choice leading to less spreading will allow the evolution to be reliable for a longer time since the boundary values will remain small longer and finite size effects will set in later.

For our purpose, comparing the quantum evolution with classical equations, the choice of initial wave packet is not that important since it is sufficient to know the evolution for limited amounts of time only. We will not be able to compare whole solutions as functions of time in this way, but since the classical equations and also the corrected ones are local in time we can see growing deviations. One can then decide which correction terms are needed to describe the local change in volume following from the quantum evolution.

A quantitative statement about the deviations is complicated by the fact that the quantum evolution is not uniquely related to a classical expression. One can take expectation values and compare with the classical functions, but due to the spread of the probability distribution the result depends on whether we take, e.g., the expectation value

$$\langle\hat{V}\rangle(t) = ||\psi_t||^{-2}\sum_{j=1}^{N} v_{m_c-N/2+j}|\psi_{t,j}|^2 \tag{16}$$

of the volume operator or that of the scale factor operator $\hat{a} = \hat{V}^{1/3}$ and the third power afterwards. Classically, we have $V = a^3$, but this relation will certainly not be satisfied for the expectation values once the spread of the wave function becomes larger (see Fig. 1, with the wave function shown in Fig. 2).

There are different sources for departures between the expectation values and classical behavior. Besides approximations used in the method to solve the constraint, there are

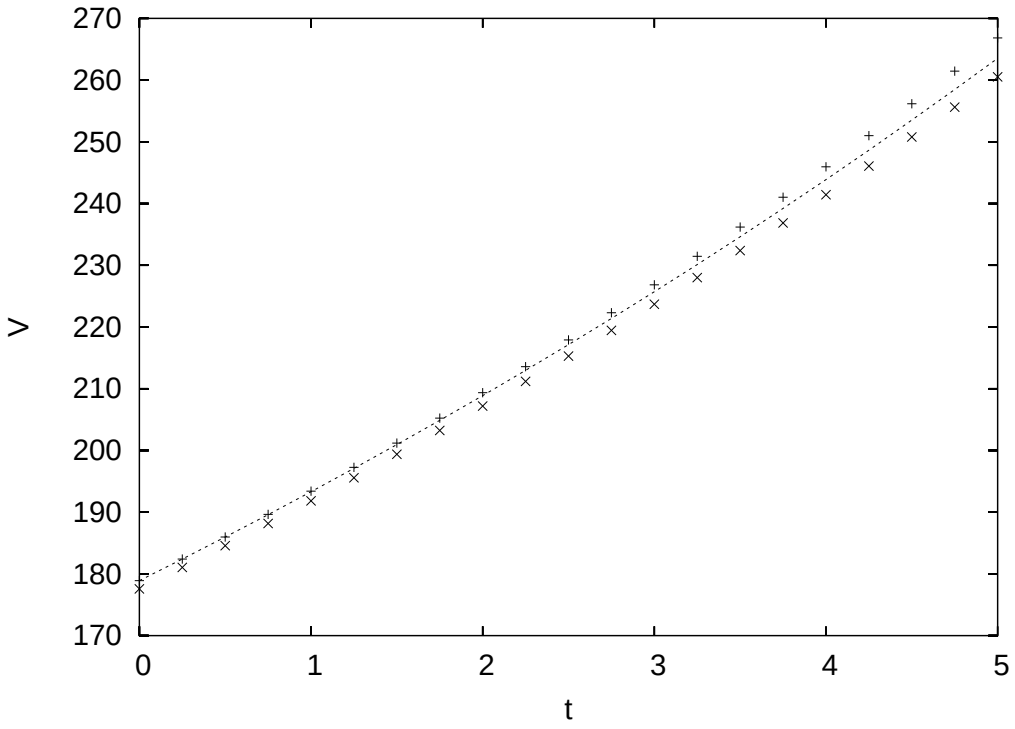

FIG. 1: Expectation value of the volume (+) compared to the classical solution $V(t)$ (dashed) and the volume $\langle\hat{a}\rangle^3(t)$ computed from the expectation value of the scale factor ($\times$) with a cosmological constant $\Lambda = 10^{-3}$ and an initial peak around $m_c = 200$ ($N = 500$, $\sigma = 20$).

quantum effects which we are most interested in here. They can be divided into two classes, the first one arising from small-scale or high-curvature effects in quantum operators, the second one coming from the fact that we have an evolving wave packet rather than a sharp classical point. Both effects can be included into effective classical equations, but in the second case it is not always clear if modifications to the classical behavior are a consequence of having chosen a bad initial state or a physical effect related to the evolution of spread, asymmetry and other deformations in profile of the probability distribution.

In order to quantify this, one can evaluate the skewness of the wavefunction as it evolves. The skewness which is initially zero for the Gaussian coherent state describes the asymmetry of the wave packet and is given in terms of various expectation values of powers of $\hat{p} = \hat{V}^{2/3}$ as

$$s = \frac{1}{\tilde{\sigma}^3}\left[\langle\hat{p}^3\rangle - 3\,\langle\hat{p}\rangle\,\langle\hat{p}^2\rangle + 2\langle\hat{p}\rangle^3\right] \tag{17}$$

where $\tilde{\sigma}$ is the standard deviation $(\langle\hat{p}^2\rangle - \langle\hat{p}\rangle^2)^{1/2}$ which initially is given by $\tilde{\sigma}_{\rm in} = \frac{2}{3}\gamma\sigma$. (We

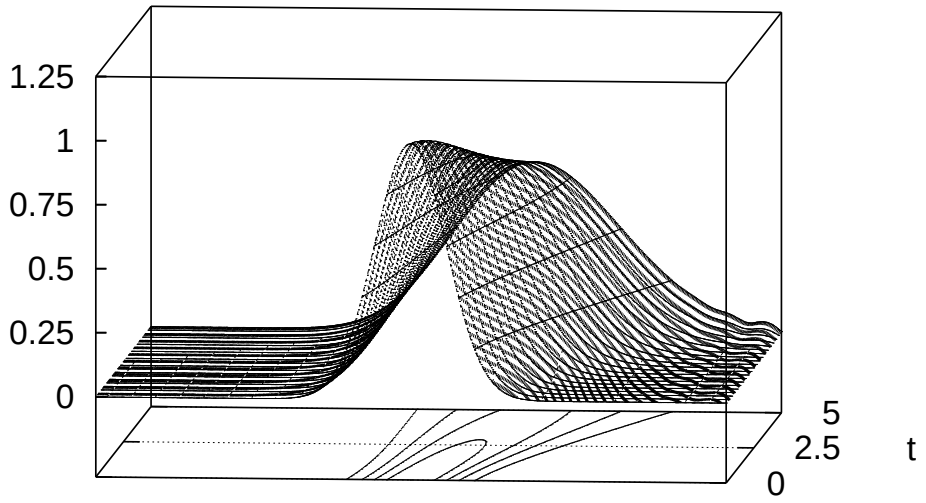

FIG. 2: A spreading wave packet for $\Lambda = 10^{-3}$ as in Fig. 1. At the back of the right hand side one can see small oscillations building up when the wave reaches the boundary. The vertical axis shows the magnitude of the normalized wave function, which starts as a Gaussian at the front and evolves to the back.

use $\hat{p}$ in order to define skewness because it is the isotropic component of the densitized triad, which is basic in loop quantum gravity. Eigenvalues of $\hat{p}$ are proportional to μ or m such that the skewness is computed for the variable in the wave function.). It is clear from Fig. 3 that the initial Gaussian wave packet gets skewed with time and deforms, but that the deformation remains small such that the main parameters characterizing the wave packet in the cases studied here are only its expectation value and spread.

The evolution of skewness with time reflects that the coherent state is no more peaked at its classical value, which is one cause of departure between quantum and classical curves. Fig. 3 shows the spread of the wavefunction with respect to its initial value. A symmetric spreading would give an evolved coherent state still peaking at classical values at late times for the operator $\hat{a}^2$ corresponding to the discrete argument m of the wave function. The

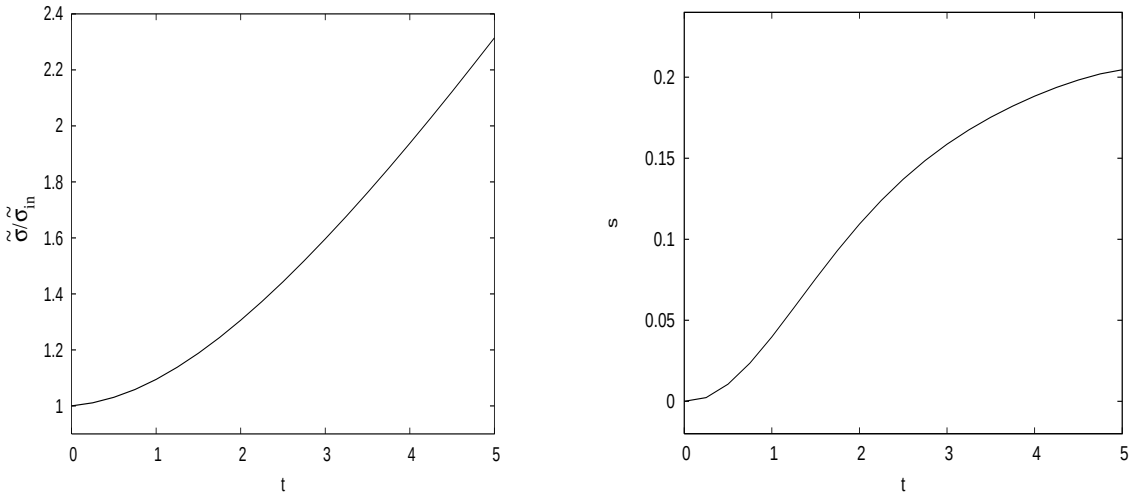

FIG. 3: Growth of standard deviation and skewness for the case in Fig. 1.

significance of small growth in skewness for the time scale of interest is that the probability distribution of the wavefunction remains peaked close to the classical volume. Since the quantized volume and scale factor are given by powers of m different from one, they do not follow the classical curve exactly, their difference increasing with increasing spread and skewness.

2. Accelerated expansion

A more interesting example is given by dust as matter content, which we use to model effective densities as derived in [34] and based on expressions of the full theory [35]. This is the main ingredient for effective classical equations with the most dramatic effects, and the methods developed here allow us to put this term in effective equations on a more solid footing.

To that end we replace the classical matter energy density for dust, $\rho(a) = M/a^3$ with a constant M, by $\rho(a) = M d_{j,l}(a)$ with the effective density

$$d_{j,l}(a) = a^{-3} D_l(3a^2/\gamma j \ell_{\rm P}^2) \tag{18}$$

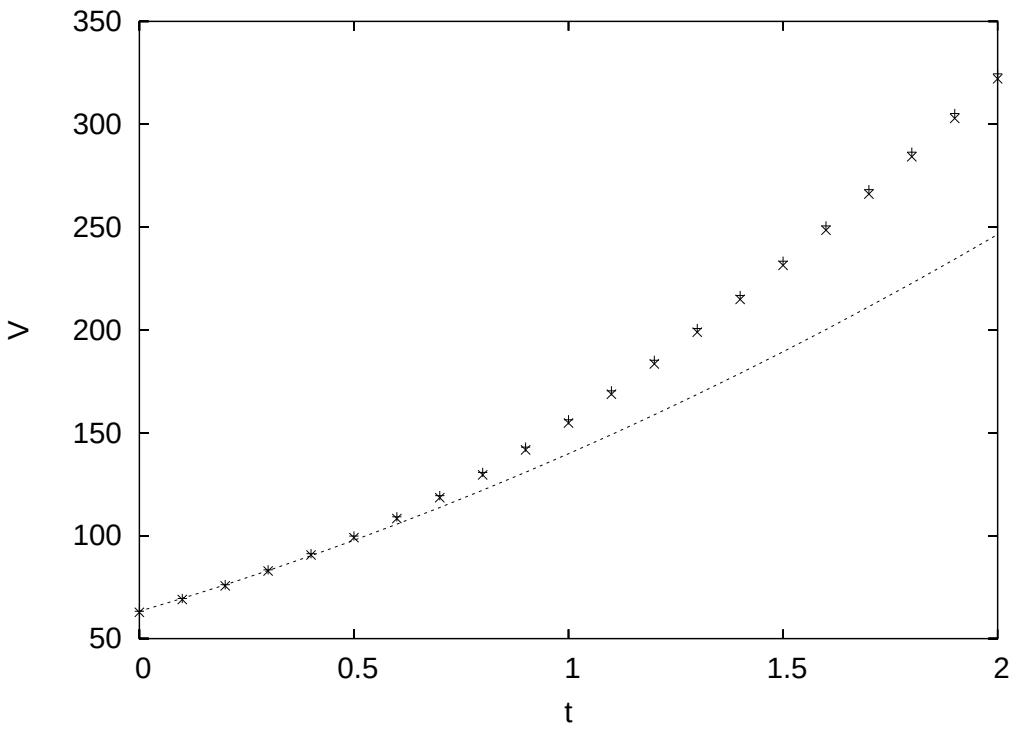

FIG. 4: Expectation value of the volume (+) compared to the classical solution $V(t)$ and the volume computed from the expectation value of the triad (×) for dust with $M = 10$ and an initial peak around $m_c = 100$ ($N = 1000$, $\sigma = 20$). The ambiguity parameter j for the effective density is $j = 400$, such that the density peaks at $m_* \approx j/2 = 200$ corresponding to a volume $V_* = (2\gamma\ell_{\rm P}^2 m_*/3)^{3/2} \approx 180\ell_{\rm P}^3$, which is reached around $t = 1.1$.

where

$$D_l(q) \;=\; q^{3/2}\left\{\frac{3}{2l}\left(\frac{1}{l+2}\left[(q+1)^{l+2}-|q-1|^{l+2}\right]\right.\right.$$
$$\left.\left.-\;\frac{q}{l+1}\left[(q+1)^{l+1}-\mathrm{sgn}(q-1)|q-1|^{l+1}\right]\right)\right\}^{3/(2-2l)} \tag{19}$$

and j is a quantization ambiguity parameter (a half-integer) [34]. There is another ambiguity parameter $0 < l < 1$ [2], which is more restricted by full loop quantum gravity and is usually taken as $l = 3/4$. For very small $a \ll \sqrt{j}\ell_{\rm P}$, $d_{j,l}(a)$ behaves as a positive power of a,

$$d_{j,l}(a) \sim \left(\frac{3}{l+1}\right)^{3/(2-2l)} (3a^2/\gamma\ell_{\rm P}^2 j)^{3(2-l)/(2-2l)} a^{-3} \tag{20}$$

i.e.

$$d_j(a) := d_{j,\frac{3}{4}}(a) \sim \left(\frac{12}{7}\right)^6 (\tfrac{1}{3}\gamma\ell_{\rm P}^2 j)^{-15/2} a^{12}\,. \tag{21}$$

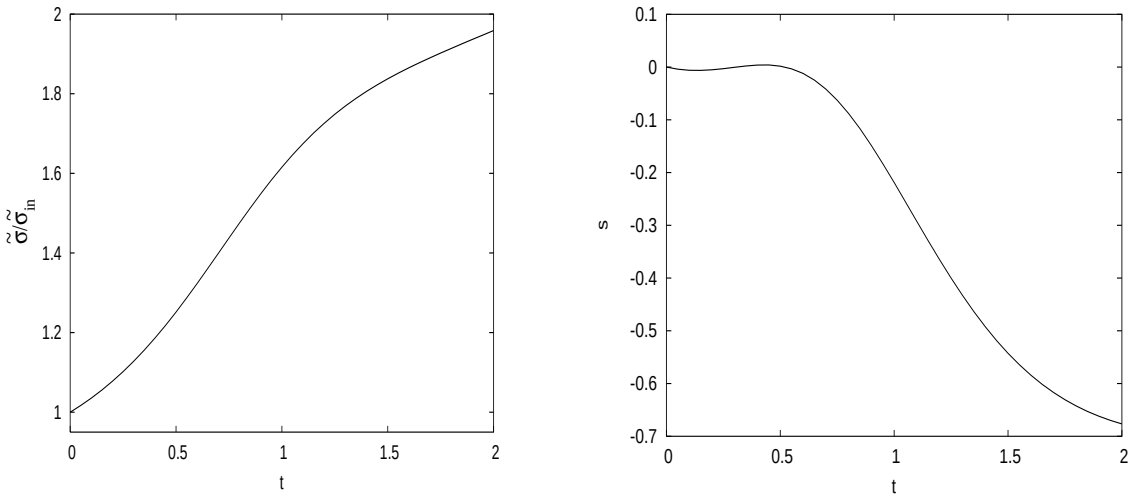

FIG. 5: The evolution of standard deviation and skewness for the case in Fig. 4. The spread increases most strongly in the inflationary regime, while the wave packet is skewed stronger during unaccelerated expansion.

We emphasize that for dust this is not the matter density most naturally expected from loop quantum gravity. Rather, in loop quantum gravity the matter Hamiltonian is primary and will be quantized. Since this is a constant M for dust, there would be no modifications of this kind at all to the classical equations. We use the modification (which can also be interpreted as arising from an additional quantization ambiguity [11, 45]) here to model the kinetic term of a scalar Hamiltonian, and in order to study the implications of effective densities.

That the effective density modifies not only the classical evolution but also the quantum dynamics can be seen in Fig. 4. The volume expectation value increases more strongly than the classical solution, which unlike in Fig. 1 is not an effect of a spreading wave packet or skewness: Fig. 5 shows that spreading and skewness are not large. This is also depicted in Fig. 6 which shows the wave packet which does not spread strongly during the displayed evolution.

Moreover, the expectation value of the volume operator agrees better with the cubic power of the expectation value of the scale factor than with the classical solution, which is another sign that the modified dynamics is responsible for the deviations, rather than just change in shape of wave packet. However, Fig. 4 does not tell us decisively how well the expectation values would agree with modified classical dynamics. A hallmark of the effective

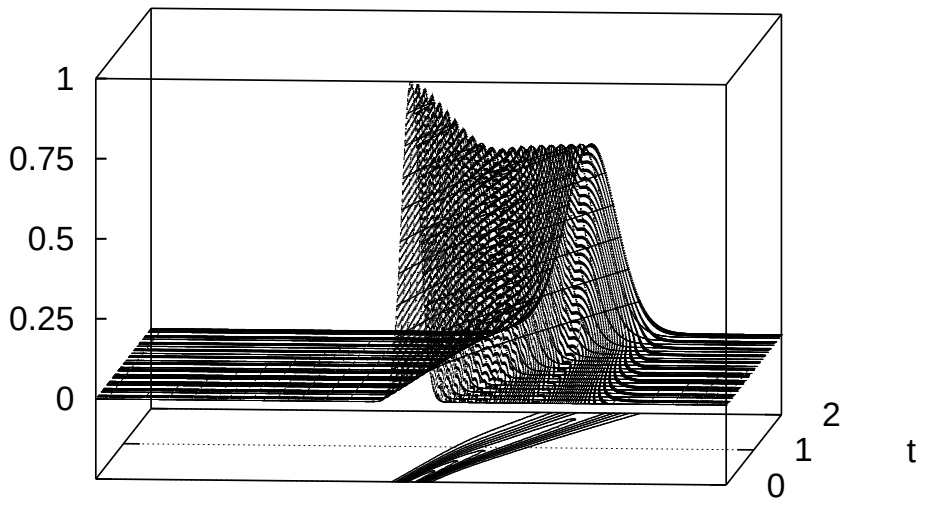

FIG. 6: A spreading wave packet $|\psi_{t,i}|$ for the evolution of Fig. 4.

density $d_j(a)$ is that it implies inflation when inserted into the classical equations and when the scale factor is below the peak value. In fact, the expectation values in Fig. 4 increase more strongly than the classical solution, but in the range $0 < t < 1.1$, where we are below the peak, deviations are small.

It is much more illuminating to plot time derivatives, or rather difference quotients from the numerically obtained data, and compare with the classical behavior. Fig. 7 shows that in fact the derivative of the scale factor increases when $t < 1.1$, i.e. below the peak of $d_j(a)$, and thus accelerates in agreement with the expectation.

In order to check the effective density more directly we compare the expectation values to numerical solutions of the effective classical equation with the matter density replaced by $Md_j(a)$. Fig. 8 shows that indeed the effective solution is much closer to the expectation values than the unmodified classical solution. Also the derivative of the scale factor in Fig. 10 agrees well with the change of the expectation values in the regimes before and after the peak. In particular, the inflationary behavior in the modified region with increasing $\dot{a}$

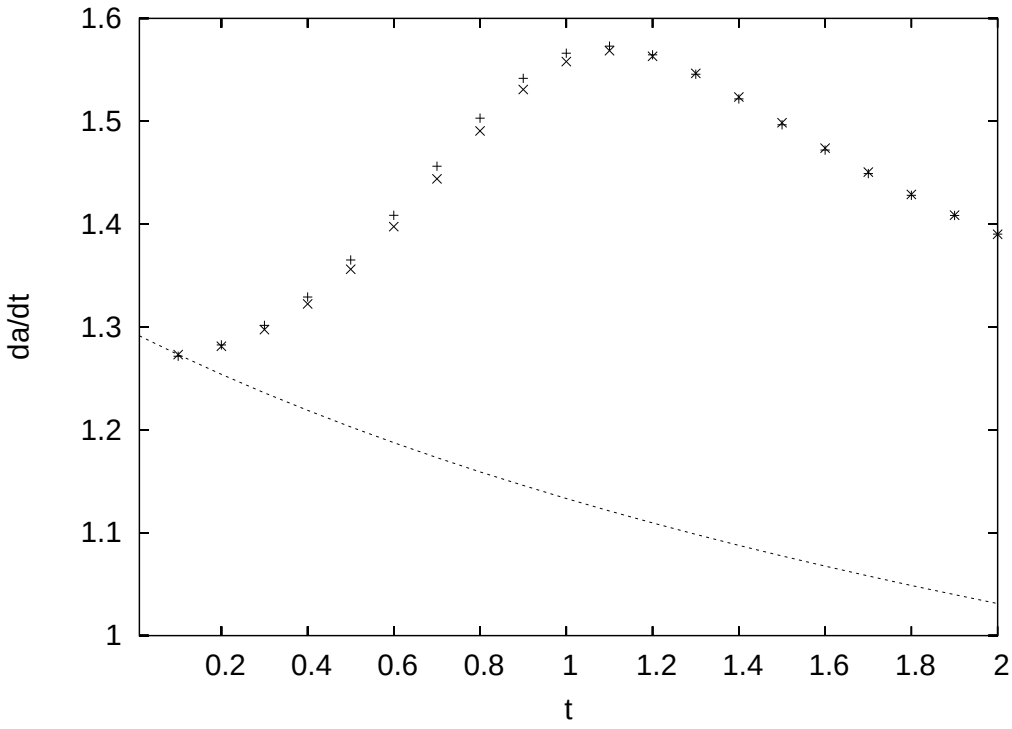

FIG. 7: Time derivative of scale factors plotted in Fig. 4.

can be seen from the classical as well as quantum solution. After the peak, both show the expected non-inflationary behavior.

However, around the peak the effective classical time derivative is larger than the change in expectation values, which is also the reason why the effective classical volume is slightly larger than the quantum volume at later times in Fig. 8. At this point, $\dot{a}$ is largest so that higher order corrections (higher powers of $\dot{a}$ in the Friedmann equation) are expected to have the strongest influence. Those corrections have not yet been included into effective classical equations and we leave a more detailed investigation of their effect around the peak for future work. Nevertheless, one can see numerically that in the case studied here the effect of higher order terms is negligible. This can also be seen from the fact that those higher order terms arise as powers in $c = -\frac{1}{2}\gamma\dot{a}$ which thanks to the smallness of γ remains sufficiently small compared to one throughout the evolution. Moreover, for the flat model the Hamiltonian is invariant under change of sign in c such that the next higher order correction is suppressed by a power c^2.

Rather, the reduced derivative of the scale factor around the peak is a consequence of deformations of the wave packet as shown in Fig. 9. In fact, around the peak the effective

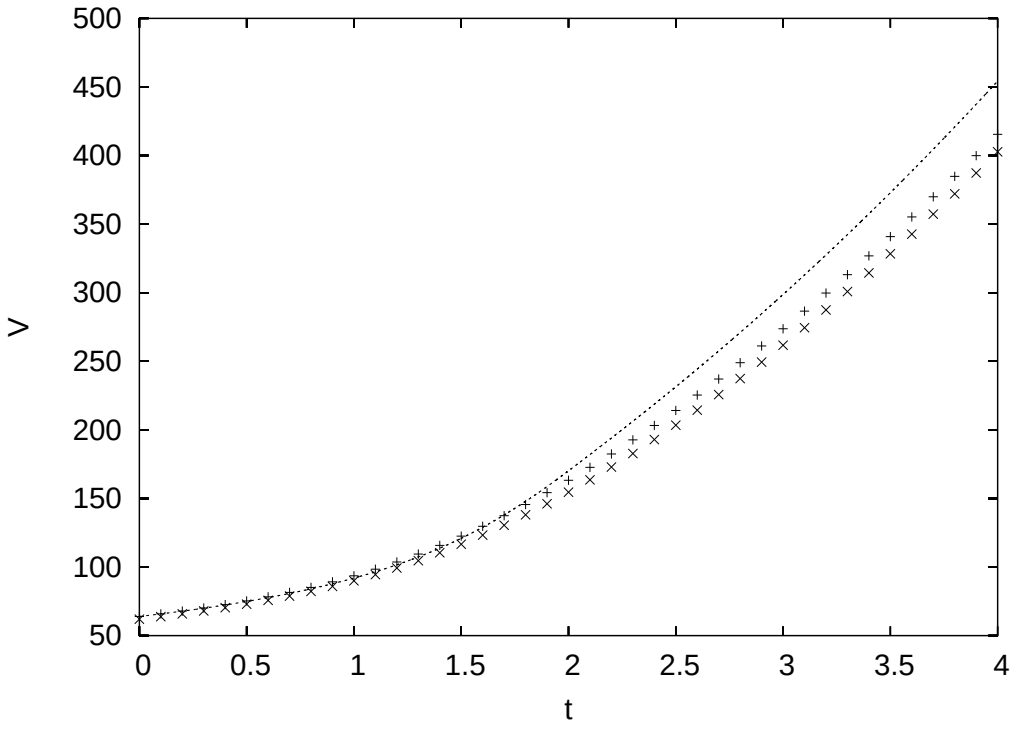

FIG. 8: Volume expectation values compared to the effective classical solution. Compared to the points in Fig. 4 the quantum behavior is different since the initial wave packet is now peaked on the effective rather than unmodified classical constraint surface (which decreases the initial c_0).

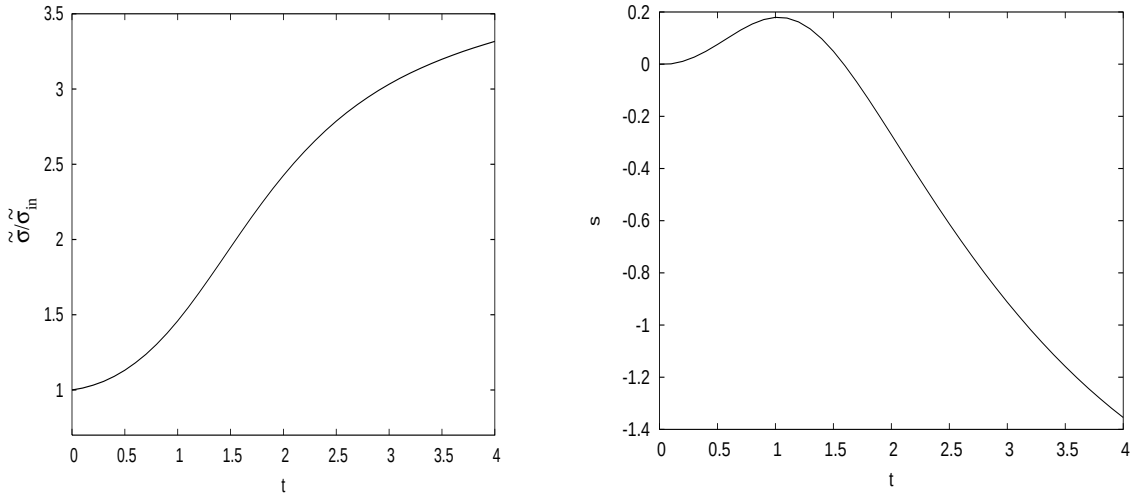

FIG. 9: The time variation of standard deviation and skewness for the matter with effective density.

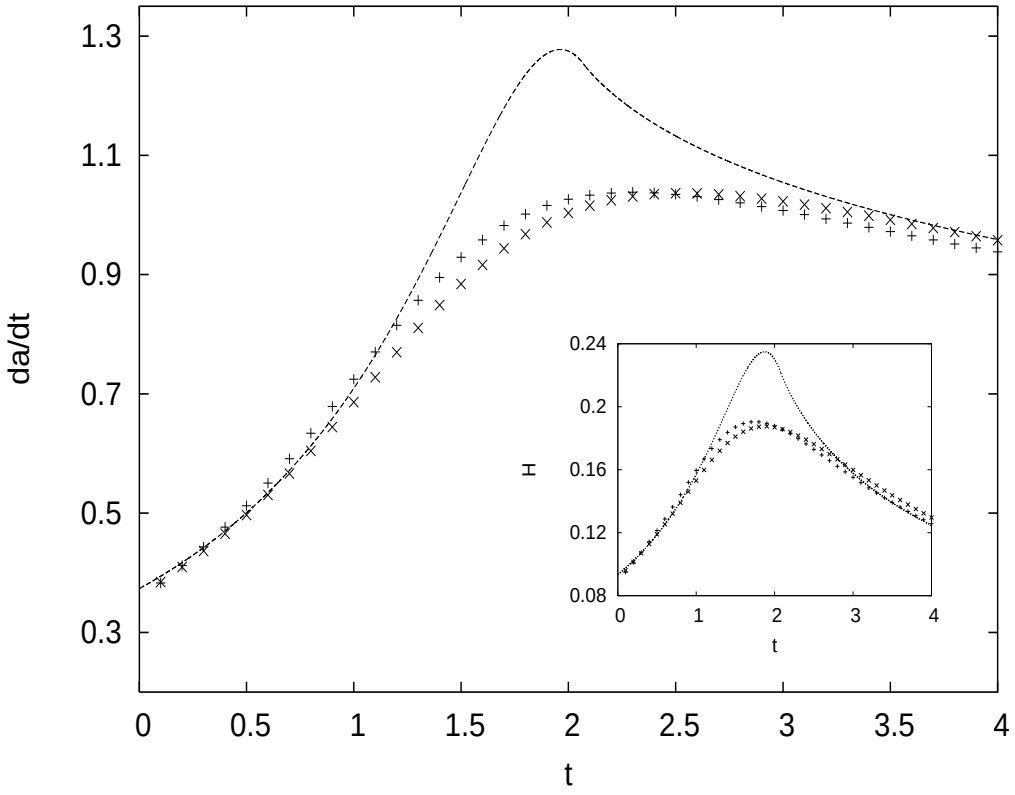

FIG. 10: Time derivative of scale factors plotted in Fig. 8. Inset shows variation of Hubble rate with time.

density changes rather rapidly from increasing to decreasing behavior. Thus, a part of the wave packet will already be in the decreasing regime while its center is still in the increasing one, which lowers the overall density seen by the wave. This behavior is verified by looking at the skewness of the wave packet during the evolution in Fig. 9. First, the skewness turns positive which means that the right tail of the wave packet becomes heavier than the left one. At some point, skewness starts to decrease and reaches negative values, describing a redistribution of parts of the wave packet such that now the left tail becomes more pronounced. This redistribution implies that expectation values of powers of m, such as the scale factor and volume, are lowered as compared to the expected evolution. In fact, comparing Fig. 9 with Fig. 10 shows that the turn-around of skewness starts just when the deviations between the change of $\langle\hat{a}\rangle$ and the effective $\dot{a}$ appear, with the expectation values increasing less strongly then the effective classical value.

This observation shows that effective classical equations used so far do not capture all

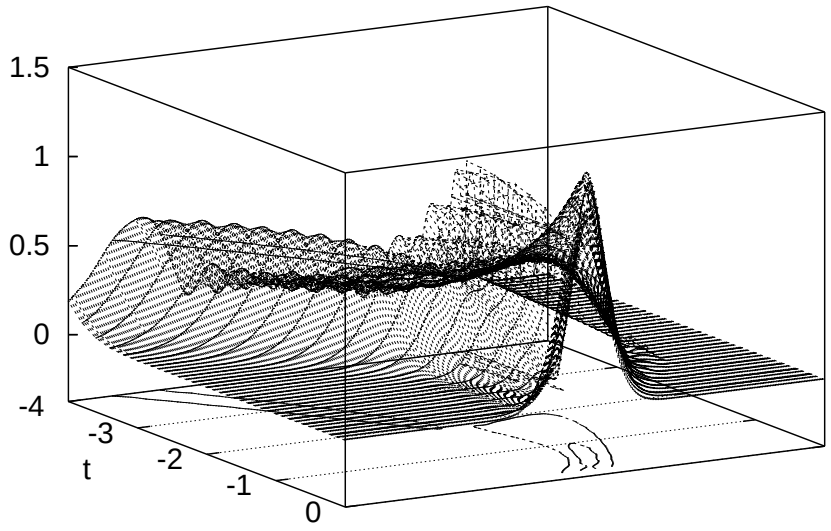

FIG. 11: Wave packet evolving toward the classical singularity and bouncing off, only penetrating negligibly to negative m. The parameters are $m_c = 100$, $N = 500$, $\sigma = 10$, $M = 10$, $j = 200$.

details in the quantum evolution around the peak. On the other hand, the behavior before and after the peak is described very well. Cosmological studies so far have mainly focused on the modified behavior at small scale factors and the initial inflationary epoch, which is modeled reliably by using just the effective density. The peak behavior was actually more problematic since the Hubble parameter in the case of scalar dynamics easily became dangerously high, larger than one in terms of Planck units, which leads to doubt in the further semi-classical evolution. Here, the quantum behavior with smaller $\dot{a}$ suggests that additional effects from the wave packet can lead to a better semi-classical picture, which may be modeled in effective classical equations by taking into account effects of skewing wave packets. How this appears in the case of a scalar field, and whether in this case $\dot{a}$ can become large enough for higher order corrections to be relevant, remains to be studied.

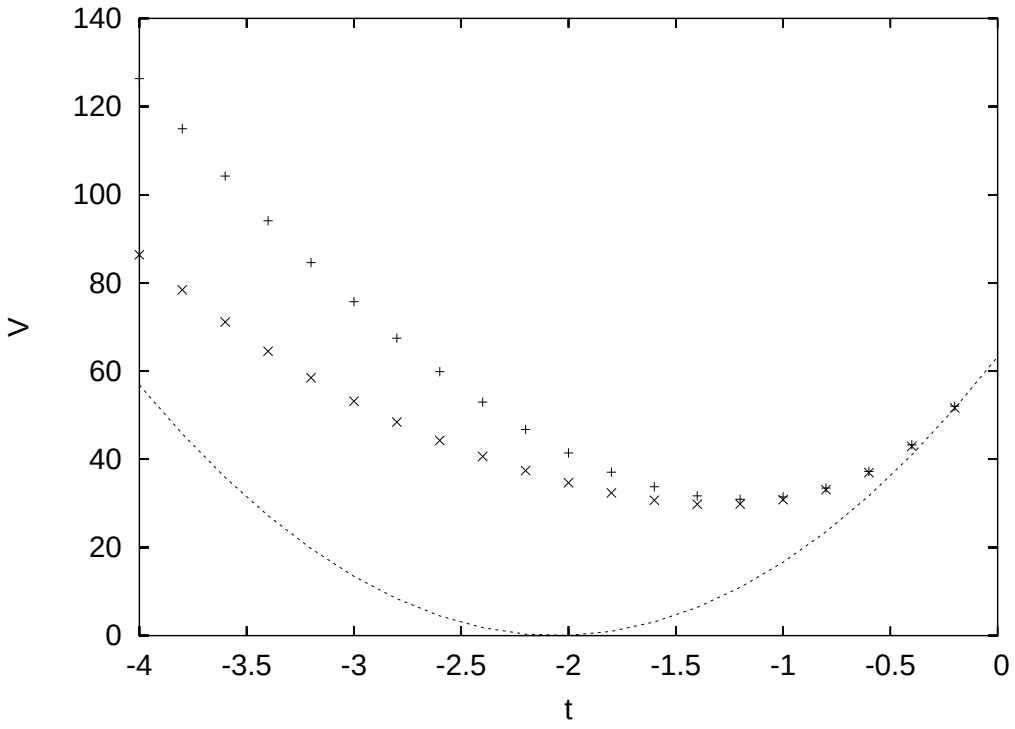

FIG. 12: Volume expectation values for the wave packet in Fig. 11. The expectation values bounce at non-zero values, while the classical curve runs into a singularity at zero volume.

3. Bounces

So far we only looked at the evolution for rather large volume. For smaller $|m|$, the approximation by classical evolution will become worse and eventually break down. When exactly this is happening depends on the parameters for the cosmological model and the choice of initial wave function. As an example we again use the dust model but evolve to earlier times, towards the classical singularity. Fig. 11 shows that the wave packet deforms once a significant part of it reaches $m = 0$. If we compute the expectation values of geometrical quantities then a bounce is observed, as demonstrated by Fig. 12.

It should be noted that the effective classical equations of a flat model do not allow a bounce even when we use the effective density in the dust case, and thus this bounce is not of the semiclassical type as in [13, 14, 15, 16, 17]. Further, deformations of the wave function show directly that the classical space-time picture is not valid during the bounce phase. Moreover, the nature of a wave packet as opposed to sharp classical values becomes more relevant, which provides a quantitative explanation of the observed bounce: The spread σ

implies a correction to the Friedmann equation which then takes the form [25]

$$\dot{a}^2 + \tfrac{1}{4}\gamma^{-2}\sigma^{-2} = \tfrac{2}{3}a^2\rho(a) \tag{22}$$

where for simplicity we ignore the a-dependence of σ due to spreading. Using the small-a approximation (21) for $d_j(a)$ in $\rho(a) = Md_j(a)$ and setting $\dot{a} = 0$ for the bounce results in a bouncing scale factor (in Planck units)

$$a_{\rm bounce} \sim 3^{-25/28}\,(\tfrac{7}{4})^{3/7}\left(\tfrac{1}{8}\sigma^{-2}M^{-1}\gamma^{11/2}j^{15/2}\right)^{1/14} \approx 2.44\,. \tag{23}$$

Since we used the small-a approximation, which overestimates $d_j(a)$, the bounce value is slightly larger resulting in $a_{\rm bounce} \approx 2.50$ if the function $d_j(a)$ is used without approximation. The corresponding bounce volume, $V_{\rm bounce} \approx 15.6$ is considerably smaller than the minimum expectation value in Fig. 12. But if we use the effective Friedmann equation (22) to place the initial wave packet on the effective constraint surface the expected bounce radius and the numerical one in Fig. 13 agree within the limits of the expectation values $\langle\hat{V}\rangle$ and $\langle\hat{a}\rangle^3$. In fact, the wave packet bounces earlier than expected classically, but around the expected volume. Thus, the spread-dependent correction term explains why there is a bounce and gives a good approximation for the bounce radius.

Nevertheless, it is also clear from Fig. 13 that the agreement between the expectation values and the effective solution deteriorates around the bounce. This can also be seen from Fig. 14, which shows considerable change in spread of the wavefunction. In fact, the wave packet does not only spread but also separates into different packets as seen in Fig. 15. Thus, even taking into account the spread dependence in the modified Friedmann equation would not completely describe the quantum behavior. (Note that the spread dependent correction term was derived under the assumption of a Gaussian wave packet. Fig. 14 also shows that the skewness does not increase strongly, but for this case of a wave separating into different packets skewness alone is not a good measure for the deviations from a Gaussian.) The evolution can then no longer be seen as semiclassical and it is not possible to get a better agreement by including further corrections into a classical equation.

Still, one can also see that there is a rather undisturbed wave packet bouncing off, while other parts of the wave function stay around the classical singularity which does not affect expectation values of geometrical quantities very much. Thus during the evolution shown here the expectation value of the volume and the cube of that of the scale factor do not

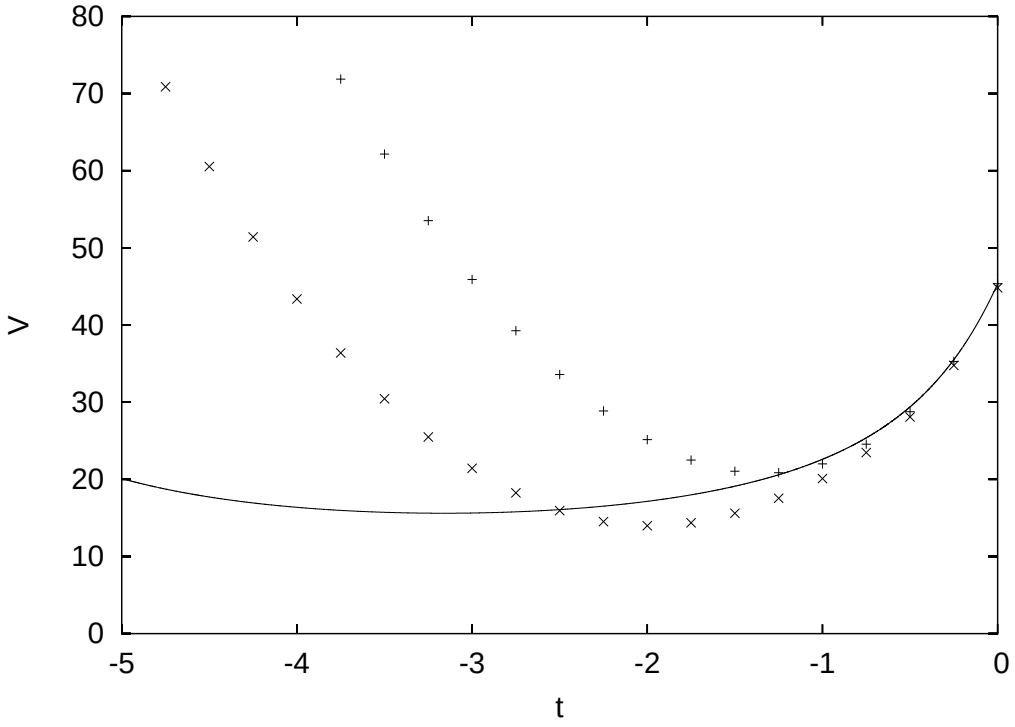

FIG. 13: Volume expectation values for the wave packet initially peaked at the effective constraint surface compared to a numerical solution of the effective Friedmann equation (22). Since the corresponding wave packet, plotted in Fig. 15, moves closer to the classical singularity than in Fig. 11, the spread increases faster than in Fig. 12.

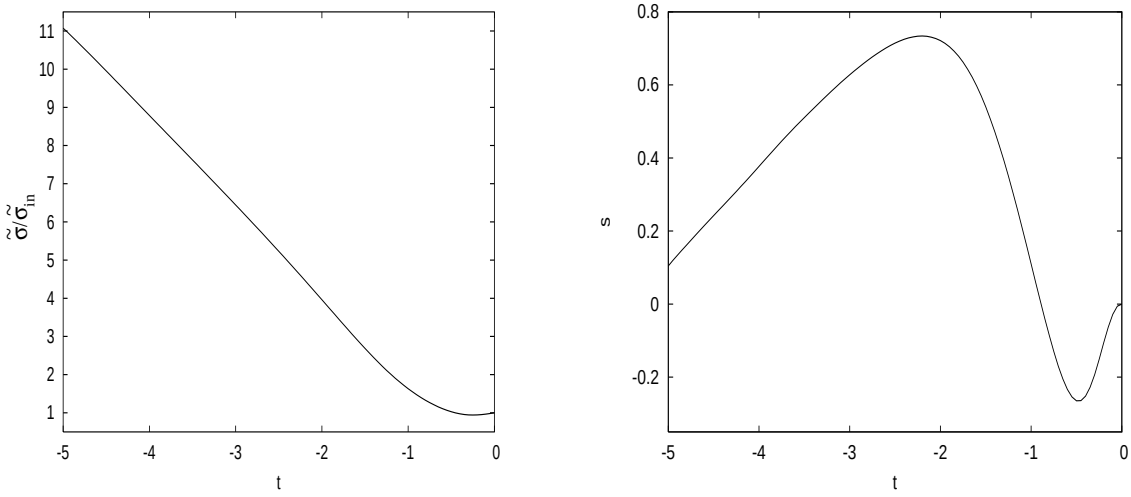

FIG. 14: Increase in spread and skewness for backward evolution through a bounce as in Fig. 13.

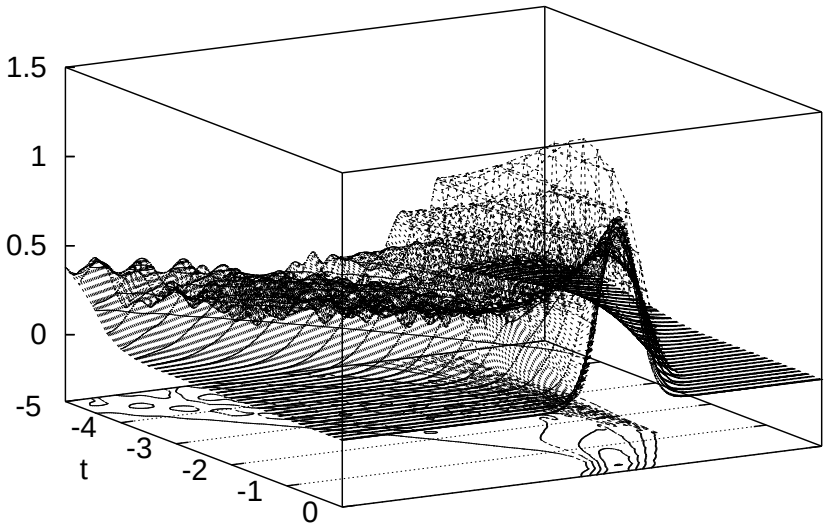

FIG. 15: Wave packet evolving toward the classical singularity and bouncing off as in Fig. 11, but initially peaked on the effective constraint surface at $m_c = 80$. Since the bounce radius now is smaller, the leakage to negative m is larger (see rightmost contour line).

deviate too much near the classical singularity. However, since strong oscillations build up rapidly, there are strong curvature fluctuations. This is shown in Fig. 16, where the fluctuations of $\dot{a}$, computed from the $\dot{a}$-operator

$$(\hat{\dot{a}}\ \psi)_m = \tfrac{1}{2} i\gamma^{-1}(\psi_{m+1} - \psi_{m-1})\,, \tag{24}$$

which initially are smaller than $\dot{a}$ increase to have a maximum at the bounce. After the bounce, curvature fluctuations decrease but stay larger than initially, and are comparable to the value of $\dot{a}$ in Fig. 17. We thus can still think of semiclassical spatial slices of a certain volume at least in early stages of the bounce, but since the extrinsic curvature is not sharp one cannot think of them as forming a classical, smooth space-time.

If, as before, we compute the time derivative of the expectation value of the scale factor, rather than the expectation value of curvature, it is still increasing, i.e. accelerates, as a consequence of the effective density (Fig. 17). This figure also shows that the expectation value of the $\dot{a}$-operator (24) follows the change of $\langle\hat{a}\rangle$ more closely than the effective clas-

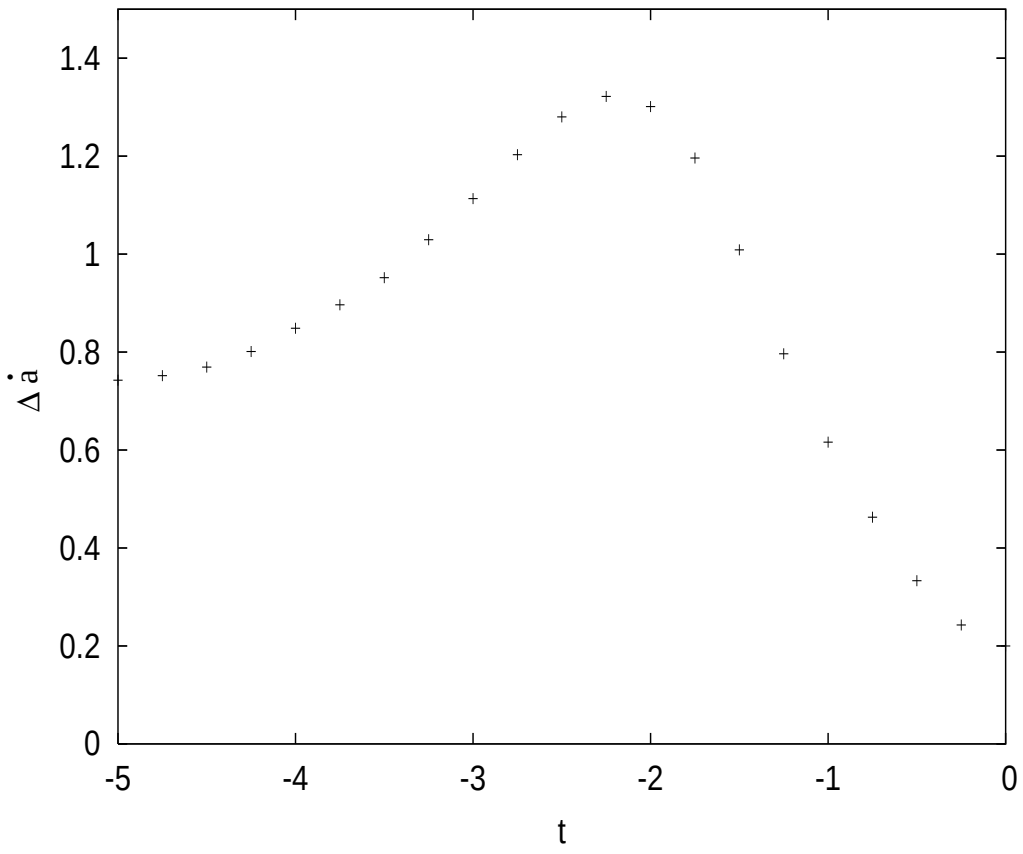

FIG. 16: Extrinsic curvature fluctuation $\Delta\dot{a} = \sqrt{\langle(\hat{\dot{a}})^2\rangle - \langle\hat{\dot{a}}\rangle^2}$ corresponding to Fig. 13 where the operator for $\dot{a}$ is derived from the c-operator mapping a state ψ_m to $\frac{1}{4}i(\psi_{m+1} - \psi_{m-1})$.

sical solution, which implies that the interpretation of extrinsic curvature (computed from the geometrical quantity a as compared to connection components) has an unambiguous meaning.

As seen in Fig. 15, the wave function leaks only slightly into the part of minisuperspace corresponding to negative m (i.e. the part corresponding to the side beyond the classical singularity in the internal time formulation [8, 46]). This is another reason for the fact that we can still approximately speak of a classical bounce of the volume. If the wave function at negative m would be larger, also the spread in spatial geometrical quantities and not just in extrinsic curvature would be large and classical geometry would break down completely. Whether or not this is happening depends very sensitively on detailed quantization choices in the Hamiltonian constraint and initial values of the wave function (see also [38, 40, 47]).

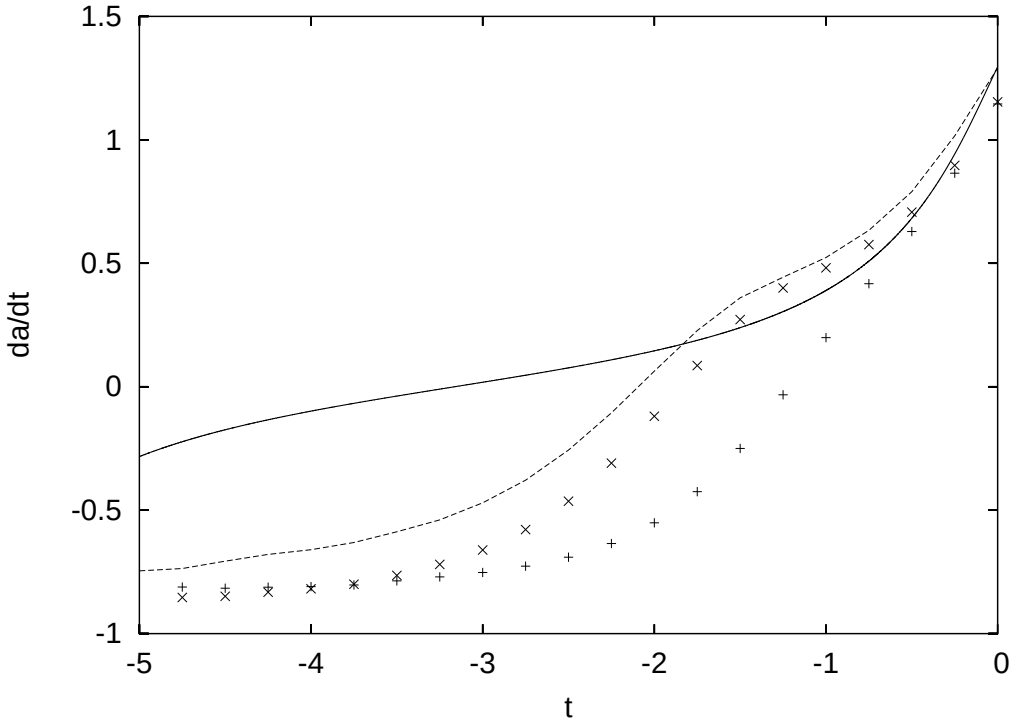

FIG. 17: Time derivative of the scale factor expectation values in Fig. 13 compared to the effective solution. The dashed line connects expectation values $\langle\hat{\hat{a}}\rangle$.

V. CONCLUSIONS

Group averaging allows to introduce a coordinate time parameter into quantum gravity, although only in an approximate sense. Still, the resulting evolution equations are helpful in semiclassical analysis and in providing intuitive pictures of quantum effects.

Our main application in this paper is a justification of using effective densities as the most prominent quantum gravity effect imported into effective classical equations. As it turns out, the modified classical equations describe the quantum evolution of wave packets very well, down to surprisingly small scales. Stronger deviations become noticeable only when the wave packet starts to touch the classical singularity. When exactly this happens depends on details of the model and the chosen initial state. The diverse effects giving rise to departures from classical behavior can be separated by varying the parameters involved in the models. For instance, we chose rather large values for the ambiguity parameter j determining the peak of the effective density, in order to distinguish this effect from that of perturbative corrections. In this way it is possible to study each correction term in the

effective Hamiltonian separately.

The replacement of classically diverging factors of a^{-3} in dynamical equations by a bounded effective density $d(a)$ has been confirmed as the main effect. Effective densities themselves are partly responsible for this observation since, via the effective Friedmann equation, they lead to a reduction of extrinsic curvature $\dot{a}$. This means that higher order corrections, i.e. higher powers of $\dot{a}$, are less relevant at small a than without effective densities. Visible effects then occur most likely around the peak of the effective density, where $\dot{a}$ is largest. As observed here, the quantum Hubble rate is in fact smaller than would be expected just from the effective density, which is helpful for cosmological applications. However, numerically one can check that in the cases studied here the reduced Hubble rate is a consequence of deformations of the wave packet, parameterized here by the skewness, rather than of higher order terms. Such an effect would have to be included in effective classical equations by introducing a correction term depending on the skewness of an evolving wave packet. That it is possible to describe the influence of properties of wave packets on the evolution by effective classical equations has been demonstrated here by studying bounces implied by a spread dependent correction term. The corresponding correction for skewness, however, is not known since in the derivations of correction terms so far Gaussian states with zero skewness have been used [25]. For cosmological purposes it would be interesting to apply this technique to the case of a scalar field and study the role played by effective densities in particular around the peak.

Detailed formulas for perturbative correction terms, which include higher order and higher derivative corrections, and uncertainty correction terms related to the spread of the wave function, are currently being evaluated. Once available, they can be used for a direct comparison with the quantum evolution as studied here. In particular the uncertainty corrections, which are proportional to σ^{-2} [25], play a role at small volume since, unlike higher order corrections, they are not suppressed by effective densities. An application of this correction term can be found in studying bounces, where it provides an explanation for the bounce in Fig. 11 which does not follow from effective densities alone. The approximate expression of the bounce radius (23) determines the scale where quantum effects from the wave packet become important, indicated by correction terms depending on the spread σ. For a phenomenological analysis, a_{bounce} can be used as initial value of the scale factor, which is relevant for estimates of the amount of inflation. Since the value derived here for dust

depends on all the parameters of the model, in particular the ambiguity parameter j, it is clear that the analysis will be more complicated than the original ones, where the initial scale factor was assumed to be $a_{\rm initial} = \sqrt{\gamma}\ell_{\rm P}$. With an expression like $a_{\rm bounce}$, more reliable estimates can be made and constraints on the parameters can be tightened. Thanks to the strong initial increase of $d(a)$ with a, which is responsible for the small power 1/14 in (23), the dependence on parameters of the model is, fortunately, rather weak.

At very small scales the evolution of wave packets shows when the classical space-time picture can be trusted, when it needs to be corrected and when it breaks down completely. In this regime the evolution becomes much more sensitive to quantization choices in the Hamiltonian constraint. In particular this is true for the leakage into the domain of negative m, where the orientation of space is reversed, which is not surprising since this corresponds to evolution beyond the classical singularity in the internal time picture. In this context one should note that we had to use a symmetric ordering of the constraint in order to apply group averaging and for the coordinate time evolution to be numerically stable. This ordering already implies changes to the issue of initial conditions [48] and on the relation between the wave function at positive and at negative m. The alternative procedure of using a lapse function $N(t) = a(t)$ and quantizing NH symmetrically, as mentioned in Sec. IV A, also changes the issue of initial conditions since the lapse vanishes at the classical singularity and the wave function at negative m completely decouples from that at positive m. Thus, while the coordinate time picture is well suited to justifying effective classical equations at non-vanishing volume, the issue of the classical singularity can be understood only by using the wave function directly and thus employing an internal time to formulate evolution. Since the classical space-time picture breaks down in this regime, there is no analog to coordinate time.

Acknowledgments

PS thanks Max-Planck-Institut für Gravitationsphysik for supporting a visit and warm hospitality during early stage of this work. His work is supported in part by Eberly research

funds of Penn State and by NSF grant PHY-00-90091.

---

[1] M. Bojowald and H. A. Morales-Técotl, Cosmological applications of loop quantum gravity, In *Proceedings of the Fifth Mexican School (DGFM): The Early Universe and Observational Cosmology*, Lect. Notes Phys. 646 (2004) 421–462 (Springer-Verlag), [gr-qc/0306008]

[2] M. Bojowald, Loop Quantum Cosmology: Recent Progress, In *Proceedings of the International Conference on Gravitation and Cosmology (ICGC 2004), Cochin, India*. Pramana (2004) to appear, [gr-qc/0402053]

[3] M. Bojowald, Inflation from quantum geometry, *Phys. Rev. Lett.* 89 (2002) 261301, [gr-qc/0206054]

[4] M. Bojowald and K. Vandersloot, Loop quantum cosmology, boundary proposals, and inflation, *Phys. Rev. D* 67 (2003) 124023, [gr-qc/0303072]

[5] G. Date and G. M. Hossain, Effective Hamiltonian for Isotropic Loop Quantum Cosmology, [gr-qc/0407073]

[6] M. Bojowald, G. Date, and K. Vandersloot, Homogeneous loop quantum cosmology: The role of the spin connection, *Class. Quantum Grav.* 21 (2004) 1253–1278, [gr-qc/0311004]

[7] M. Bojowald, Loop Quantum Cosmology IV: Discrete Time Evolution, *Class. Quantum Grav.* 18 (2001) 1071–1088, [gr-qc/0008053]

[8] M. Bojowald, Isotropic Loop Quantum Cosmology, *Class. Quantum Grav.* 19 (2002) 2717–2741, [gr-qc/0202077]

[9] M. Bojowald, Homogeneous loop quantum cosmology, *Class. Quantum Grav.* 20 (2003) 2595–2615, [gr-qc/0303073]

[10] S. Tsujikawa, P. Singh, and R. Maartens, Loop quantum gravity effects on inflation and the CMB, [astro-ph/0311015]

[11] M. Bojowald, J. E. Lidsey, D. J. Mulryne, P. Singh, and R. Tavakol, Inflationary Cosmology and Quantization Ambiguities in Semi-Classical Loop Quantum Gravity, *Phys. Rev. D* to appear, [gr-qc/0403106]

[12] G. Date and G. M. Hossain, Genericity of inflation in isotropic loop quantum cosmology, [gr-qc/0407069]

[13] P. Singh and A. Toporensky, Big Crunch Avoidance in k = 1 Semi-Classical Loop Quantum

Cosmology, *Phys. Rev. D* 69 (2004) 104008, [gr-qc/0312110]

[14] M. Bojowald, R. Maartens, and P. Singh, Loop Quantum Gravity and the Cyclic Universe, [hep-th/0407115]

[15] J. E. Lidsey, D. J. Mulryne, N. J. Nunes, and R. Tavakol, Oscillatory Universes in Loop Quantum Cosmology and Initial Conditions for Inflation, [gr-qc/0406042]

[16] G. V. Vereshchagin, Qualitative Approach to Semi-Classical Loop Quantum Cosmology, *JCAP* 07 (2004) 013, [gr-qc/0406108]

[17] G. Date and G. M. Hossain, Genericity of Big Bounce in isotropic loop quantum cosmology, [gr-qc/0407074]

[18] M. Bojowald and G. Date, Quantum suppression of the generic chaotic behavior close to cosmological singularities, *Phys. Rev. Lett.* 92 (2004) 071302, [gr-qc/0311003]

[19] M. Bojowald, G. Date, and G. M. Hossain, The Bianchi IX model in loop quantum cosmology, *Class. Quantum Grav.* 21 (2004) 3541–3569, [gr-qc/0404039]

[20] P. G. Bergmann, Observables in General Relativity, *Rev. Mod. Phys.* 33 (1961) 510–514

[21] K. V. Kuchař, Time and interpretations of quantum gravity, In G. Kunstatter, D. E. Vincent, and J. G. Williams, editors, *Proceedings of the 4th Canadian Conference on General Relativity and Relativistic Astrophysics* (World Scientific: Singapore, 1992)

[22] C. Rovelli, Time in Quantum Gravity: An Hypothesis, *Phys. Rev. D* 43 (1991) 442–456

[23] D. Marolf, Refined Algebraic Quantization: Systems with a Single Constraint, gr-qc/9508015

[24] A. Ashtekar, M. Bojowald, and J. Lewandowski, Mathematical structure of loop quantum cosmology, *Adv. Theor. Math. Phys.* 7 (2003) 233–268, [gr-qc/0304074]

[25] A. Ashtekar, M. Bojowald, and J. Willis, in preparation

[26] A. Ashtekar, J. Lewandowski, D. Marolf, J. Mourão, and T. Thiemann, Quantization of Diffeomorphism Invariant Theories of Connections with Local Degrees of Freedom, *J. Math. Phys.* 36 (1995) 6456–6493, [gr-qc/9504018]

[27] T. Thiemann, Quantum Spin Dynamics (QSD), *Class. Quantum Grav.* 15 (1998) 839–873, [gr-qc/9606089]

[28] T. Thiemann, Quantum Spin Dynamics (QSD) II: The Kernel of the Wheeler-DeWitt Constraint Operator, *Class. Quantum Grav.* 15 (1998) 875–905, [gr-qc/9606090]

[29] T. Thiemann, QSD III: Quantum Constraint Algebra and Physical Scalar Product in Quantum General Relativity, *Class. Quantum Grav.* 15 (1998) 1207–1247, [gr-qc/9705017]

[30] T. Thiemann, The Phoenix Project: Master Constraint Programme for Loop Quantum Gravity, [gr-qc/0305080]

[31] J. Lewandowski and D. Marolf, Loop Constraints: A Habitat and their Algebra, *Int. J. Mod. Phys. D* 7 (1998) 299–330, [gr-qc/9710016]; R. Gambini, J. Lewandowski, D. Marolf, and J. Pullin, On the Consistency of the Constraint Algebra in Spin Network Quantum Gravity, *Int. J. Mod. Phys. D* 7 (1998) 97–109, [gr-qc/9710018]

[32] M. Bojowald and H. A. Kastrup, Symmetry Reduction for Quantized Diffeomorphism Invariant Theories of Connections, *Class. Quantum Grav.* 17 (2000) 3009–3043, [hep-th/9907042]

[33] M. Bojowald, Inverse Scale Factor in Isotropic Quantum Geometry, *Phys. Rev. D* 64 (2001) 084018, [gr-qc/0105067]

[34] M. Bojowald, Quantization ambiguities in isotropic quantum geometry, *Class. Quantum Grav.* 19 (2002) 5113–5130, [gr-qc/0206053]

[35] T. Thiemann, QSD V: Quantum Gravity as the Natural Regulator of Matter Quantum Field Theories, *Class. Quantum Grav.* 15 (1998) 1281–1314, [gr-qc/9705019]

[36] M. Bojowald and G. Date, Consistency conditions for fundamentally discrete theories, *Class. Quantum Grav.* 21 (2004) 121–143, [gr-qc/0307083]

[37] D. Cartin, G. Khanna, and M. Bojowald, Generating function techniques for loop quantum cosmology, *Class. Quantum Grav.* (2004) to appear, [gr-qc/0405126]

[38] F. Hinterleitner and S. Major, Isotropic Loop Quantum Cosmology with Matter II: The Lorentzian Constraint, *Phys. Rev. D* 68 (2003) 124023, [gr-qc/0309035]

[39] M. Bojowald and F. Hinterleitner, Isotropic loop quantum cosmology with matter, *Phys. Rev. D* 66 (2002) 104003, [gr-qc/0207038]

[40] D. Green and W. Unruh, Difficulties with Closed Isotropic Loop Quantum Cosmology, [gr-qc/0408074]

[41] M. Domagala and J. Lewandowski, Black hole entropy from Quantum Geometry, [gr-qc/0407051]; K. A. Meissner, Black hole entropy in Loop Quantum Gravity, [gr-qc/0407052]

[42] A. Ashtekar, J. C. Baez, A. Corichi, and K. Krasnov, Quantum Geometry and Black Hole Entropy, *Phys. Rev. Lett.* 80 (1998) 904–907, [gr-qc/9710007]

[43] A. Ashtekar, J. C. Baez, and K. Krasnov, Quantum Geometry of Isolated Horizons and Black Hole Entropy, *Adv. Theor. Math. Phys.* 4 (2001) 1–94, [gr-qc/0005126]

[44] J. M. Velhinho, Comments on the kinematical structure of loop quantum cosmology, *Class. Quantum Grav.* 21 (2004) L109–L113, [gr-qc/0406008]

[45] G. M. Hossain, Hubble operator in isotropic loop quantum cosmology, *Class. Quantum Grav.* 21 (2004) 179–196, [gr-qc/0308014]

[46] M. Bojowald, Absence of a Singularity in Loop Quantum Cosmology, *Phys. Rev. Lett.* 86 (2001) 5227–5230, [gr-qc/0102069]

[47] M. Bojowald and K. Vandersloot, Loop Quantum Cosmology and Boundary Proposals, In *Xth Marcel Grossmann meeting*, 2003, [gr-qc/0312103]

[48] M. Bojowald, Dynamical Initial Conditions in Quantum Cosmology, *Phys. Rev. Lett.* 87 (2001) 121301, [gr-qc/0104072]; Initial Conditions for a Universe, *Gen. Rel. Grav.* 35 (2003) 1877–1883, [gr-qc/0305069]

[49] The loop quantization of the symmetry reduced cosmological model from the full theory is done in such a way that the scale factor as used here (which is related to the cubic root of the volume of the fiducial cell necessary to define symplectic structure) is invariant to its conventional rescaling freedom in classical cosmology. For details see Ref. [24].